Perturbed-angular-correlation study of static and dynamic quadrupole interactions in the Laves-phase hydrides HfV$_2$H$_x$

M. Forker, W. Herz, D. Simon, and S. C. Bedi*

Institut für Strahlen-und Kernphysik der Universität Bonn, Nussallee 14-16, D-53115 Bonn, Germany

(Received 28 December 1994)

The static and dynamic electric quadrupole interaction (QI) of the nuclear probe ^{111}Cd on V sites of the C15 Laves-phase HfV$_2$H$_x$ has been systematically investigated as a function of temperature ($10 \leq T \leq 600$ K) and hydrogen concentration ($0 \leq x \leq 3.8$) by perturbed-angular-correlation (PAC) measurements. Previous ^{111}Cd PAC measurements in unloaded HfV$_2$ by Jain *et al.* have revealed an unexpected increase of the QI with temperature up to 900 K. In this work high-temperature PAC measurements have established that this anomalous temperature dependence of the QI continues up to the melting point of HfV$_2$ and further provide evidence for a high-temperature transformation of the MgCu$_2$ structure. The room-temperature quadrupole frequency v_q in the hydrides α-HfV$_2$H$_x$ increases with the hydrogen concentration x. The increase can be approximated by two linear functions with a drastic change of slope at $x \approx 1.5$: $(\delta \ln v_q / \delta T)_{x=0.0} \approx 0.2$ and $(\delta \ln v_q / \delta T)_{x=1.5} \approx 1.1$, respectively. This observation can be related to the high density of V d states at the Fermi energy in the concentration range $0 \leq x \leq 1.5$ and suggests that the p-valence electrons are the dominant source of the electric-field gradient at the V site. The variation of the QI in α-HfV$_2$H$_x$ with temperature depends sensitively on the hydrogen concentration x: For $x \leq 1.5$ and $T \geq 300$ K one finds the same anomalous increase $\delta \ln v_q / \delta T > 0$ as in unloaded HfV$_2$, whereas at higher concentrations the QI shows the decrease $\delta \ln v_q / \delta T < 0$ usually found in metallic systems. This unusual temperature dependence of the QI possibly reflects a thermal repopulation of Fermi-surface electrons, an interpretation supported by the observation that the range of the anomaly $\delta \ln v_q / \delta T > 0$ coincides with a region of high, rapidly decreasing density of states in the band structure of HfV$_2$. The activation energy E_a for hydrogen jumps in HfV$_2$H$_x$, derived from the dynamical damping of the PAC spectra in the fast-fluctuation regime, shows a maximum at intermediate concentrations $x \approx 1.5$, which is partially in conflict with NMR results for $E_a(x)$.

I. INTRODUCTION

The cubic C15 Laves phases ZrV$_2$ and HfV$_2$ have been extensively investigated in recent years because of their interesting superconducting and electronic properties on the one hand[1-9] and their pronounced hydrogen storage capacity on the other hand.[10-13]

Valuable contributions to the present state of knowledge on these compounds are due to hyperfine spectroscopic techniques. The electronic structure and its changes upon hydrogenation has been investigated by NMR measurements of Knight shifts and relaxation rates.[14-19] The NMR technique has also been used to determine the activation energies of the hydrogen diffusion in ZrV$_2$ and HfV$_2$ hydrides.[16,17,19] The occupation of the hydrogen sites in ZrV$_2$H$_x$ has been studied by measurements of muon-spin precession.[20]

The static and dynamic properties of the electric-field gradient (EFG) in ZrV$_2$ and HfV$_2$ and some of their hydrides have been investigated by ^{2}D and ^{51}V NMR (Refs. 21–24) and ^{181}Ta perturbed-angular-correlation (PAC) measurements[25,26] of electric quadrupole interactions (QI). These studies, aiming at information on the low-temperature structural instability of these compounds, the hydrogen dynamics, and the effect of the hydrogenation on the EFG were mostly performed at or below room temperature and data on the QI at higher tempera-

tures have only recently become available.[27-29]

The investigation of the QI at higher temperatures, carried out by ^{111}Cd PAC spectroscopy, led to a surprising observation.[27] The quadrupole frequency v_q of the PAC probe ^{111}Cd on the V site of HfV$_2$ increases strongly with increasing temperature. This increase—by more than 20% between 300 and 900 K—is in striking contrast to the temperature trend observed in practically all metallic systems investigated up to now, where the quadrupole frequency decreases with increasing temperature[30] which is usually attributed to the combined effect of lattice expansion and thermal vibrations.[31]

In this paper we report an extension of the QI studies from HfV$_2$ to its hydride system, motivated by the observation that—contrary to HfV$_2$—the QI of ^{111}Cd in the C15 hydride HfV$_2$H$_{3.8}$ presents a normal temperature dependence with $\delta \ln v_q / \delta T < 0$.[28] Band-structure calculations for the C15 Laves phases[7,8] show that in the case of ZrV$_2$ and HfV$_2$ the Fermi level falls into a sharp peak in the density-of-states (DOS) curve $N(E)$ and predict a pronounced decrease of $N(E_f)$ if the Fermi energy is shifted upwards by rigid-band-like filling of the DOS with electrons introduced by hydrogenation. This prediction has been experimentally confirmed by measurements of the Knight shift, the magnetic susceptibility and the specific heat.[17,18,32] In HfV$_2$H$_x$ and ZrV$_2$H$_x$ the DOS at the Fermi level $N(E_f)$ decreases by almost one order of

    <u>51</u>   15 994

magnitude from the peak at $x = 0$ towards a valley at $x > 1.5$, so that HfV_2 and $HfV_2H_{3.8}$ differ strongly in their $N(E_f)$ values.

This clearly raises the question of a correlation between the anomaly $\delta \ln v_q / \delta T > 0$ of the QI and the large DOS $N(E_f)$ of HfV_2 which could be answered by a measurement of $\delta \ln v_q / \delta T$ as a function of $N(E_f)$. The broad homogeneity range of HfV_2H_x offers the opportunity for such an experiment. HfV_2H_x maintains the $C15$ lattice structure of HfV_2 (for $T \ge 310$ K) up to hydrogen concentrations of $x \approx 4$. Hydrogenation of HfV_2 to different concentrations therefore allows a controlled, continuous variation of the $N(E_f)$ value from the peak to the valley of the DOS without affecting the symmetry of the metal lattice. Measurements of $\delta \ln v_q / \delta T$ at different hydrogen concentrations could therefore provide information on the influence of the DOS at the Fermi energy on the EFG and its temperature dependence and extend our present, still limited understanding of the EFG in noncubic metals and alloys.

For these reasons we have carried out a systematic investigation of the ^{111}Cd QI at the V site in the Laves-phase hydrides HfV_2H_x as a function of temperature (20 K $\le T \le 600$ K) at different hydrogen concentrations ($0 \le x \le 4$) by PAC spectroscopy. In addition, these measurements provide data on the phase diagrams of the Hf-V and the HfV_2-H systems and also on the hydrogen diffusion in HfV_2H_x, in particular the activation energies E_a for hydrogen jumps at different hydrogen concentrations. The NMR results reported by different authors for the concentration dependence of the activation energies in HfV_2H_x and ZrV_2H_x are partially conflicting[16,17,19] and measurements of $E_a(x)$ by different techniques are therefore of interest.

II. SOME BASIC PROPERTIES OF HfV_2 AND ITS HYDRIDES HfV_2H_x

The Laves-phase HfV_2 is the only intermetallic compound in the Hf-V phase diagram.[33] It melts congruently, with the reported melting point varying between 1820 K (Ref. 34) and 1850 K.[35] At room temperature HfV_2 crystallizes in the cubic ($C15$) $MgCu_2$-type structure ($Fd3m$). According to Ref. 36, cited by Ferro and Mararzza,[37] HfV_2 is possibly polymorphic, forming—as the Laves-phase $HfCr_2$ (Refs. 35 and 37)—also a phase of $MgNi_2$-type at higher temperatures. The local symmetry of the Hf site in the $C15$ structure is cubic, that of the V site noncubic with the point space-group symmetry $3m$. Consequently the tensor $V_{ij} = \delta^2 V / \delta x_i \delta x_j$ of the electric-field gradient (EFG) is nonzero and axially symmetric at the V site, but vanishes at the Hf site. Therefore, at $T > 120$ K, an electric quadrupole interaction can only be expected for the V site. At $T \approx 120$ K a Martensitic transition leads to a low-temperature phase for which Lawson and Zachariasen[38] have proposed an orthorhombic symmetry, while more recent results by Kozhanov et al.[39] favor a tetragonal structure.

HfV_2 and ZrV_2 are easily hydrogenated. At room temperature and hydrogen pressures $p \le 1$ bar, these Laves phases may absorb more than four H atoms per formula unit. At $T \ge 300$ K, HfV_2H_x and ZrV_2H_x maintain the $C15$ lattice symmetry (α phase), with the lattice parameter a increasing continuously with the hydrogen concentration x.[11,16,17,24]

The $C15$ structure contains three types of tetrahedral interstitial sites which may accommodate the hydrogen atoms. There are 96 g sites (Wyckoff notation) formed by two V and two Hf atoms (2V/2Hf), 32 e sites (3V/1Hf), and 8 b sites (4V) per unit cell with eight HfV_2 formula units. The site occupation in ZrV_2H_x has been studied as a function of the hydrogen concentration by neutron diffraction and neutron vibrational spectroscopy.[20] For concentrations $x < 2$ the hydrogen atoms occupy only the g sites. Occupation of the e sites sets in at $x \sim 2$ and b sites are occupied only at $x > 3$.

The lattice structure at low temperatures varies with the hydrogen concentration. The information available for the ZrV_2H_x system has been collected by Hempelmann et al.[20] in a phase diagram which shows the existence of a fct β phase at $x \approx 2$, a body-centered-orthorhombic (bco) γ phase at $x \approx 3$, a fct δ phase at $x \approx 4$, and a bco ϵ phase at $x \approx 6$. Furthermore there are indications of a ζ phase at $x \approx 0.5$ and a η phase at $x \approx 1.5$. According to Belyaev et al.,[24] the β phase of the HfV_2H_x system extends from $x \approx 1$ to $x \approx 2$. The transition from the disordered α phase to the ordered δ phase (space group $I4_1/a$) in HfV_2D_4 has been investigated by Irodova et al.[13]

III. ELEMENTS OF THE PAC THEORY FOR STATIC AND DYNAMIC QUADRUPOLE INTERACTIONS IN METAL-HYDROGEN SYSTEMS

The time modulation of the angular correlation of a $\gamma\gamma$ cascade by hyperfine interactions in polycrystalline samples can be described by the perturbation factor $G_{kk}(t)$ which depends on the multipole order, symmetry, and time dependence of the interaction and on the nuclear spin of the state under consideration (see, e.g., Fauenfelder and Steffen[40]).

In this paper we are dealing with perturbations by the electric quadrupole interaction (QI) between the nuclear quadrupole moment Q and the tensor of the electric-field gradient (EFG) at the nuclear site, which is usually expressed in terms of the quadrupole frequency $v_q = eQV_{zz}/h$ and the asymmetry parameter $\eta = (V_{xx} - V_{yy})/V_{zz}$, where $V_{ii}(i = x, y, z)$ are the principal axis components of the EFG with $|V_{xx}| \le |V_{yy}| \le |V_{zz}|$.

The time dependence of the EFG seen by a nuclear probe in a metal-hydrogen system changes with temperature from static to rapidly fluctuating: In the low-temperature limit the hydrogen ions are "frozen" on the available interstitial sites and a static EFG is produced by the hydrogen ions, the metal ions and the distribution of the valence and conduction electrons. In the case of a nonstoichiometric hydride equivalent metal sites may have a different number of vacancies in surrounding hydrogen shells and consequently the ensemble of the probe nuclei is subject to an EFG distribution. For a distribu-

tion of static QI's in polycrystalline samples the perturbation factor $G_{kk}(t)$ is given by the expression

$$G_{kk}(t;\nu_q,\eta,\delta)=s_{k0}+\sum_{n=1}^{N} s_{kn}\cos(\omega_n t)$$

$$\times\exp[-1/2(\delta\omega_n t)^2] \ . \quad (1)$$

The frequencies ω_n are the transition frequencies between the hyperfine levels into which a nuclear state is split by the QI. These frequencies depend on the quadrupole frequency ν_q and the asymmetry parameter η. The amplitudes s_{kn} are functions of η only. The number of terms N depends on the nuclear spin. For ^{111}Cd with $I=5/2$ one has $N=3$. The exponential factor in the perturbation function accounts for the effect of a Gaussian EFG distribution with relative width δ. Frequently, several fractions of nuclei with different QI parameters are found in the same sample. The effective perturbation factor is then given by

$$G_{kk}(t)=\sum_i f_i G_{kk}(t;\nu_{qi},\eta_i,\delta_i) \ , \quad (2)$$

where f_i (with $\sum_i f_i=1$) is the relative intensity of the ith fraction with the QI parameters $[\nu_{qi},\eta_i,\delta_i]$.

At higher temperatures the hydrogen atoms jump among the numerous vacant interstitial sites available in a substoichiometric hydride, giving rise to fluctuations of the QI. Since most of these sites are nonequivalent with respect to a given probe site, the spin ensemble of the probe nuclei is perturbed by fluctuations between states which differ both in orientation and magnitude of the EFG components, i.e., by (anisotropic) fluctuations of a QI distribution.

The average jump rate w is given by the Arrhenius relation $w(T)=w_0\exp(-E_a/kT)$, where E_a is the activation energy for over-barrier jumps. When the jump rate has increased with temperature to the point that the residence time between jumps τ_R is of the order of the time window of the PAC probe ($\sim 10\tau_N,\tau_N=$lifetime of the nuclear state) the nuclear-spin relaxation caused by the dynamic QI becomes observable as an attenuation of the angular correlation.

The perturbation of angular correlations by discrete jumps which may involve strong changes of the interaction is most appropriately described by Blume's stochastic theory.[41,42] The computation of the perturbation function in the exact Blume formalism, however, is a very time-consuming procedure even if only few states have to be considered and it becomes rapidly intractable for a larger number of states, as encountered, e.g., in a substoichiometric hydride.

Recently it has been shown that for jumps between the states of a QI distribution the Blume theory can under certain conditions be approximated by a perturbation function which contains a single relaxation parameter λ_k:[43]

$$G_{kk}(t)=\Gamma_{kk}(t)\exp(-\lambda_k t) \ . \quad (3)$$

The validity range of this approximation and the form of the function $\Gamma_{kk}(t)$ depend on the relative magnitude of the jump rate w and the static and dynamic components

of the QI distribution.

A fluctuating QI distribution which in the low-temperature limit is described by the center frequency ν_q^0, the average asymmetry parameter η^0 and the relative width δ can be decomposed[42,43] into a static component with frequency ν_q^s and asymmetry η^s determined by the Hamiltonian of the ensemble average $\langle V\rangle=\sum_a p_a V_a$, where V_a and p_a denote the Hamiltonian and the relative intensity, respectively, of state $|a\rangle$ in the sample and fluctuating components with frequencies ν_{qa}^f and asymmetries η_a^f determined by the Hamiltonian $V_a^f=V_a-\langle V\rangle$. An averaged dynamical frequency ν_q^f and asymmetry η^f can then be defined by $\nu_q^f=\sum_a p_a\nu_{qa}^f$ and $\eta^f=\sum_a p_a\eta_a$.

Fast processes are adequately described by Eq. (3) if several jumps occur within one spin precession period ($w\gtrsim 5\nu_q^0$). The function $\Gamma_{kk}(t)$ depends on the ensemble average of the interaction. In the case of a vanishing ensemble average ($\nu_q^s=0$) one has $\Gamma_{kk}(t)=1$ and λ_k corresponds to the Abragam and Pound spin-relaxation constant λ_k^{AP},[44] which for a QI of strength ν_q^f fluctuating with rate w between N stochastic states and nuclear spin I is given by

$$\lambda_k^{AP}=(3\pi^2/5)k(k+1)[4I(I+1)-k(k+1)$$

$$-1]/[2I(2I-1)]^2$$

$$\times(\nu_q^f)^2/(Nw) \ . \quad (4)$$

For fast processes with a nonzero ensemble average ν_q^s the function $\Gamma_{kk}(t)$ in Eq. (3) has the form of the static perturbation function for the time averaged QI $[\nu_q^s,\eta^s]$ and the relaxation parameter λ_k obtained with Eq. (3) is proportional to the Abragam and Pound constant $\lambda_k=\alpha\lambda_k^{AP}$, with $\alpha\leq 1$. So, fast fluctuations with $\nu_q^s\neq 0$ lead to a static PAC pattern with exponentially decaying amplitudes. This damping decreases with increasing jump rate which corresponds to the motional narrowing of a NMR signal. The proportionality constant α which decreases with increasing ratio ν_q^s/ν_q^f depends on the details of the model used for the simulation. Therefore the analysis of fast dynamic processes based on the approximation [Eq. (3)] provides no absolute values of the quantity $(\nu_q^f)^2/(Nw)=(\nu_q^f)^2\tau_R$. However, the approximation maintains the linearity between the derived relaxation parameter and the inverse jump rate $\lambda_k\propto 1/w$. For Arrhenius processes with $w=w_0\exp(-E_a/kT)$ one then has $\ln\lambda_k\propto E_a/kT$, so that the activation energy E_a of the jump process can be correctly deduced from the temperature dependence of the single relaxation parameter λ_k, provided ν_q^f does not change much with temperature.

The relaxation caused by slow anisotropic fluctuations with $w<\nu_q^f$ and $\tau_R>\tau_N$ is adequately described by Eq. (3) only if the static component ν_q^s of the interaction is small ($\nu_q^f>\nu_q^s$). In this case the function $\Gamma_{kk}(t)$ is identical to the static perturbation factor in the absence of fluctuations [Eq. (1)] and the relaxation constant λ_k is proportional to the jump rate w: $\lambda_k=\alpha'(N-1)w$. So, in the case of slow fluctuations the exponential damping of the amplitudes of the static PAC pattern increases with increasing jump rate w. Again only the activation energy,

but not the absolute values of the residence time can be extracted from the temperature dependence of the fitted relaxation parameter λ_k; the proportionality constant α' is model dependent, but the approximation maintains the relation $\ln\lambda_k \propto -E_a/kT$ as long as $v_q^f > v_q^s$. However, when the ensemble average becomes comparable to the fluctuating components of the QI distribution ($v_q^s \gtrsim v_q^f$) the approximation produces $-d \ln\lambda_k/d(1/kT) < E_a$ and the activation energy can be seriously underestimated.

IV. SAMPLE PREPARATION AND EQUIPMENT

The PAC measurements were carried out with the 172–247 KeV cascade of ^{111}Cd which is populated in the electron-capture decay of the 2.8 d isotope ^{111}In. Radioactive samples of HfV_2 doped with about 1 ppm of ^{111}In were produced by electron gun melting of metal foils of the constituents (Hf: 10μ, purity 97.0 at. %; V: 25μ, purity 99.95 at. %), onto which the radioactivity had been deposited from a commercially available solution of ^{111}InCl$_3$. The vacuum of the electron gun was of the order of 5×10^{-6} mbar. Prior to hydrogenation the samples were annealed at about 1000 K for 2 h and subsequently slowly cooled to room temperature. In the first stage of the investigation the annealing and hydrogenation had to be carried out in a quartz tube connected to a high vacuum (HV) system with a lower pressure limit of 10^{-6} mbar. Occasionally it was found that samples, annealed in this HV system and then exposed to a H_2 atmosphere would not absorb any hydrogen, even at elevated temperatures, which probably reflects a passivation by surface oxidation of the relatively small samples (50 mg). At a later stage, an ultrahigh vacuum (UHV) system became available and samples annealed in a vacuum of 10^{-9} mbar readily absorbed hydrogen up to concentrations $x \approx 4$.

For hydrogenation the samples were exposed to a precisely known quantity of H_2 gas (purity: 99.9999 at. %), determined by measurement of the H_2 pressure in a calibrated volume. The pressure was measured with two capacitance manometers with ranges of 0–10 mbar and 0–1000 mbar, respectively. After UHV annealing, hydrogen absorption started at room temperature. For homogenization, the samples were heated in the H_2 atmosphere to 820 K for about 2 h and then slowly cooled with a rate of 5 K min^{-1} to room temperature. The hydrogen concentration was determined from the weight of the HfV_2 samples and the pressure decrease in the calibrated volume.

The lattice parameter a at room temperature was determined as a function of the hydrogen concentration by x-ray diffraction of a series of inactive hydrides prepared with the identical procedure as the ^{111}In-doped compounds. Belyaev et al.[24] have reported a strictly linear relation between the room-temperature lattice parameter and the hydrogen concentration: $a = 7.3954(16) + 0.0966(5)x$ for $0x \leq 4$. For samples prepared in the UHV system we obtained perfect agreement with the results of Belyaev et al.,[24] while samples annealed in the HV system were found to deviate slightly and unsystematically from this linear relation. Because

of these deviations and slight differences for samples with the same nominal value of x, we attribute a systematic uncertainty Δx to the hydrogen concentration of the HV samples, as calculated from the weight and the pressure decrease. This systematic error increases from $\Delta x < 0.1$ at low concentrations to $\Delta x \approx 0.2$ at $x = 4$. For the UHV samples the accuracy of the concentration is of the order of 1% for all values of x.

The PAC spectra were recorded with a four-detector setup, equipped with fast BaF_2 scintillators. Sample temperatures $T \leq 290$ K were reached with a closed-cycle He refrigerator, temperatures $T > 290$ K in a resistance-heated furnace. For measurements at $T > 290$ K the hydrides HfV_2H_x were kept in a thin quartz tube with a volume of about 0.1 cm^3, which was O-ring sealed to a valve closed after evacuating the tube at room temperature. In view of the small mass of our samples, a small volume is important in order to prevent significant changes of the concentration by desorption at higher temperatures. We preferred closing the quartz tube with a valve rather than by melting to avoid uncontrolled heating and desorption of the samples during this process. As the quadrupole frequency depends sensitively on the hydrogen concentration (see below), irreversible hydrogen losses through the valve can be easily detected by taking a room-temperature PAC spectrum after each temperature increase. For most compounds hydrogen losses set in at $T \geq 600$ K.

A PAC furnace reaching temperatures up 2300 K (Ref. 45) was used to extend the previous measurements of the QI of ^{111}Cd in HfV_2 (Ref. 27) almost to the melting point of the compound.

V. MEASUREMENTS AND RESULTS

A. The quadrupole interaction of ^{111}Cd:HfV$_2$ between 290 and 1760 K

As a first step in this investigation we have studied the question whether the unexpected, positive temperature derivative of the QI of ^{111}Cd:HfV$_2$, established in Ref. 28 up to $T = 900$ K, continues towards higher temperatures. Figure 1 shows PAC spectra of ^{111}Cd:HfV$_2$, measured between 290 and 1760 K. Clearly, the spin precession period decreases continuously with increasing temperature, reflecting a positive $\delta \ln v_q/\delta T$ up to the melting point of HfV_2.

The analysis based on Eq. (2) shows that depending on temperature the spectra contain up to three fractions with different QI parameters $[v_q, \eta, \delta]$: At low and intermediate temperatures the PAC pattern is dominated by a periodic, almost undamped modulation, reflecting a fraction f_1 of probe nuclei subject to a sharply defined axially symmetric ($\eta = 0$) QI which can be attributed (see discussion) to ^{111}Cd on substitutional V sites of HfV_2. The quadrupole frequency v_q of this fraction as a function of temperature is displayed in Fig. 2, where different symbols refer to measurements with different samples. The asymmetry parameter η is zero at all temperatures. The relative width δ of the frequency distribution is constant $\delta \approx 0.01$ up to $T \approx 1500$ K and then increases with tem-
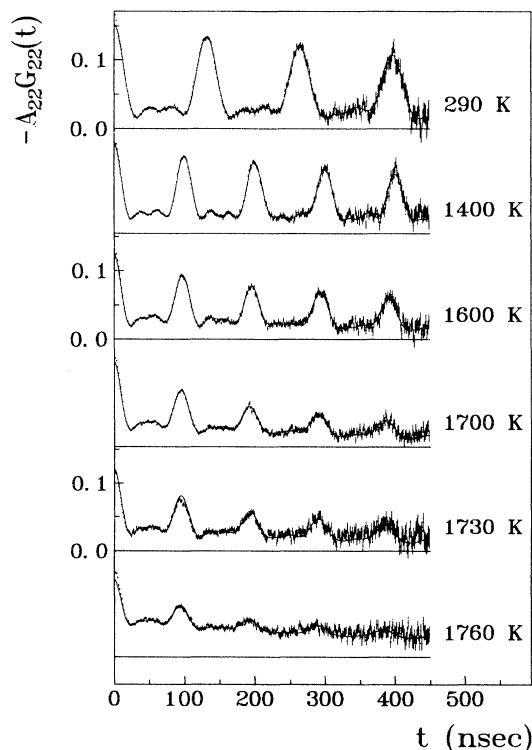
FIG. 1. PAC spectra of ^{111}Cd:HfV$_2$ at temperatures 290 K $\leq T \leq$ 1760 K.

perature to reach $\delta \approx 0.06$ at $T = 1760$ K. A second fraction with relative amplitude f_2 is required to fully describe the initial decrease of the anisotropy. The QI parameters ($v_q \approx 60-70$ MHz, $\eta \approx 0.4-0.5$, $\delta \approx 0.25-0.35$), which depend little on temperature, show that the probe nuclei in this fraction experience a broad distribution of axially asymmetric QI's centered at 60–70 MHz. The third fraction with relative intensity f_3 becomes visible at high temperatures as a shift and slight inclination of the baseline of the PAC pattern. The inclination can be equally well described by an exponential decay constant
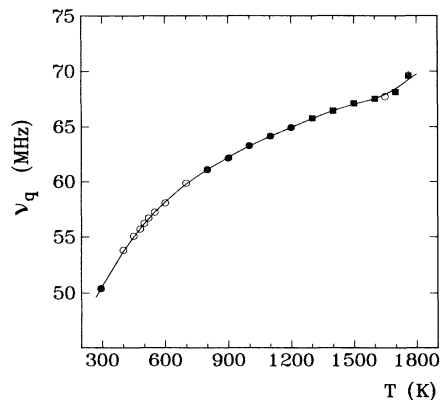

FIG. 2. The temperature dependence of the quadrupole frequency v_q of the nuclear probe ^{111}Cd on the V site of HfV$_2$. Different symbols refer to different samples.

$\lambda \sim 4$ MHz or a frequency distribution of width of $\delta v_q \sim 4$ MHz, centered at $v_q = 0$.

The temperature dependence of the f_1, f_2, and f_3 is shown in Fig. 3. The triangles and points refer to samples which were slowly heated to high temperatures, whereas the full squares show the fraction f_1 of a sample heated in one fast step from 290 to 1450 K. The open squares in Fig. 3 represent the fraction f_1 of this sample at 290 K after the measurement at temperature T.

B. The static and dynamic quadrupole interaction of ^{111}Cd:HfV$_2$H$_x$ as a function of temperature and hydrogen concentration

The static and dynamic QI of ^{111}Cd in HfV$_2$H$_x$ was studied systematically as a function of the hydrogen concentration x and the temperature T. Room-temperature PAC spectra were recorded for 33 compounds ^{111}Cd:HfV$_2$H$_x$ and the temperature dependence of the QI was determined for 22 of these samples, mostly in the temperature range 20 K $\leq T \leq$ 600 K.

Examples of characteristic spectra illustrating the typical variation of the PAC pattern with temperature and the influence of the hydrogen concentration are given in Fig. 4. These spectra and their comparison to those of unloaded HfV$_2$ (Fig. 1) show several interesting aspects. First, the sign of the temperature derivative $\delta \ln v_q / \delta T$ in the high-temperature phase $T \geq 290$ K changes with the hydrogen concentration from positive to negative: in unloaded HfV$_2$ (Fig. 1) the precision period decreases with increasing temperature, but it is almost temperature independent in HfV$_2$H$_{1.78}$ and clearly increases with temperature in HfV$_2$H$_{2.7}$ (Fig. 4). Second, at a given temperature the quadrupole frequency increases strongly with
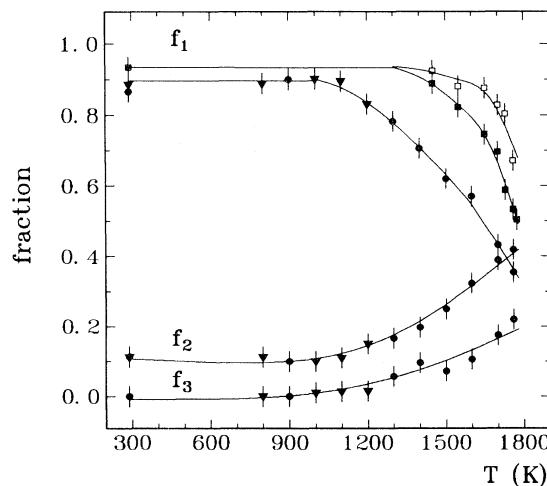

FIG. 3. The relative amplitudes f_1, f_2, f_3 of the three fractions of ^{111}Cd probes with different quadrupole parameters detected in the PAC spectra of ^{111}Cd:HfV$_2$. The full squares show the fraction f_1 of a sample heated in one rapid step from 290 to 1450 K. The open squares represent the fraction f_1 at room temperature after each high-temperature measurement of the same sample.

the hydrogen concentration, confirming the trend observed in ^{51}V and ^{2}D NMR studies of HfV$_2$H$_x$ (Refs. 27 and 24) and ZrV$_2$H$_x$ (Ref. 22) and third, as illustrated in detail by the spectra of HfV$_2$H$_{1.78}$, Fig. 4, there is clear evidence for time-dependent perturbations due to diffusing hydrogen atoms. At the lowest temperature one observes a nonperiodic, strongly attenuated PAC pattern. Since at 24 K hydrogen jumps are highly improbable within the ^{111}Cd time window, the attenuation must be the result of a static QI distribution caused by differences in the spatial arrangement of hydrogen vacancies frozen around the various PAC probes. This is confirmed by the finite anisotropy at large delay times (hard-core value). The nonperiodicity of the pattern indicates an axial asymmetry of the interaction. With increasing temperature, the spectra present the typical features of a transition from slow to fast fluctuations of a QI distribution. First there is a slight increase of the damping of the PAC amplitudes towards a minimum at 250 K, followed by a

pronounced "motional narrowing" recovery towards a periodic, almost undamped pattern, which reflects a finite ensemble average of axial symmetry (see Sec. III). From the fact that the QI precessions are never completely wiped out it may be concluded[43] that the fluctuating component v_q^f of the interaction is relatively small compared to the static ensemble average v_q^s. An estimate (see Sec. VI B) gives $v_q^f/v_q^s \leq 0.15$.

The spectra measured at 24 K were analyzed assuming a static QI. For a satisfactory description usually a superposition of two Gaussian QI distributions [Eqs. (1) and (2)] with different parameters [v_q, η, δ] and relative amplitudes $f_{1,2}$ was required. For the 24 K spectrum of HfV$_2$H$_{1.78}$ in Fig. 4 the parameters are $f_1 = 0.60$, $v_{q1} = 84$ MHz, $\eta_1 = 0.37$, $\delta_1 = 0.06$ and $f_2 = 1 - f_1 = 0.40$, $v_{q2} = 90$ MHz, $\eta_2 = 068$, $\delta_2 = 0.10$. For most other concentrations also, the frequencies of the two sites differed by less than 10%. An exception is HfV$_2$H$_{1.93}$ with $f_1 = 0.85$, $v_{q1} = 145$ MHz, and $f_2 = 0.15$, $v_{q2} = 90$ MHz at 24 K.

For temperatures $T > 24$ K dynamic perturbations by fluctuations of the QI distribution were admitted and the analysis was carried out with the approximation of a single relaxation constant discussed in Sec. III. As the description of the low-temperature measurements requires a superposition of two distributions, the dynamic perturbations were analyzed by fitting the expression

$$G_{22}(t) = [\sum_i f_i \Gamma_{22}(t; v_{qi}, \eta_i, \delta_i)] e^{-\lambda t} \tag{5}$$

with $i = 2$ and $\Gamma_{22}(t)$ given by Eq. (1) to the ^{111}Cd:HfV$_2$H$_x$ spectra. The relative intensities f_1, f_2 were fixed to the values obtained from the analysis of the 24 K spectrum, except for HfV$_2$H$_{1.93}$, where good fits were only possible with f_1 and f_2 as free parameters. Here f_1 was found to decrease from f_1 (24 K) $= 0.85$ to reach $f_1 = 0$ at $T \sim 280$ K. For the other concentrations, fits adjusting v_{qi}, η_i, and λ were performed under two assumptions: (i) the relative widths δ_i of the Gaussian QI distributions were fixed to the values at 24 K and (ii) both the relaxation parameter λ and the distribution widths δ_i were treated as free parameter which usually lead to slightly better fits but no significant difference in the value of λ. The lower part of Fig. 5 shows the relaxation parameter, the upper part the mean value δ of the distribution widths δ_i, obtained with assumption (ii). For 300 K $\leq T < 600$ K usually a single site was found to be sufficient for excellent fits to the spectra. Here both the distribution width δ and the relaxation parameter λ were treated as free parameters. The values of λ and δ for HfV$_2$H$_{1.78}$ collected in Fig. 5 show that the transition from slow to fast fluctuations occurs around 270 K. As this temperature is approached from below, the fitted distribution width decreases abruptly to almost zero, reflecting the onset of a fast averaging process. The temperature dependence of the relaxation parameter shows the Arrhenius behavior discussed in Sec. III: a linear relation of $\ln\lambda$ vs $1/T$ with a positive slope above and a negative slope below 270 K, as expected for the fast- and slow-fluctuation regime, respectively. In the slow-fluctuation region, however, the absolute value of the
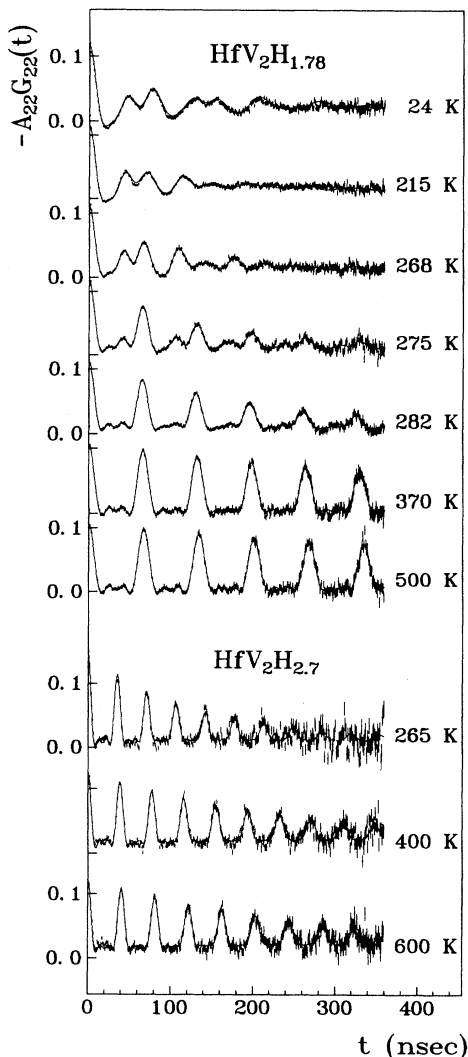

FIG. 4. PAC spectra of ^{111}Cd in the hydrides HfV$_2$H$_{1.78}$ and HfV$_2$H$_{2.7}$ at different temperatures.
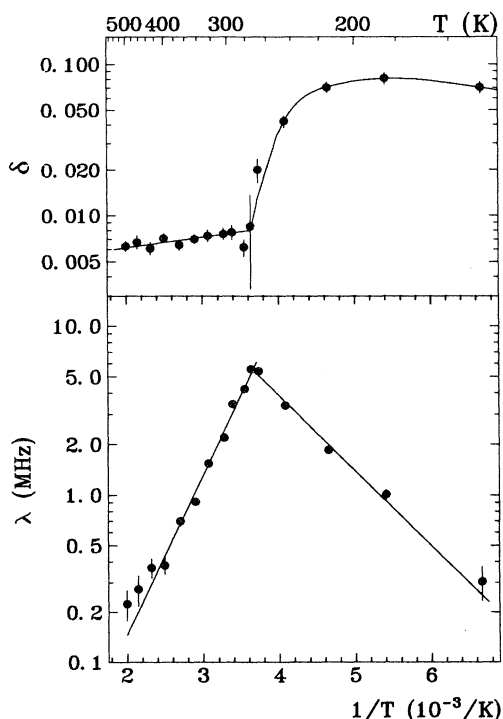
FIG. 5. The relaxation parameter λ and the relative width δ of the Gaussian frequency distribution for ^{111}Cd:HfV$_2$H$_{1.78}$ obtained from fits of Eqs. (1) and (2) to the spectra of Fig. 4.

slope is much smaller than in the fast-fluctuation region—a behavior found for all hydrogen concentrations. As pointed out in Sec. III and discussed in detail in Ref. 43, this difference which in many cases exceeds a factor of 2, is an artifact of the analysis. In the slow-fluctuation regime the approximation of a single relaxation constant fails, because in the present case the fluctuating part is much smaller than the static component of the interaction $(v_q^f/v_q^s \leq 0.15$, see Sec. VI B). Therefore
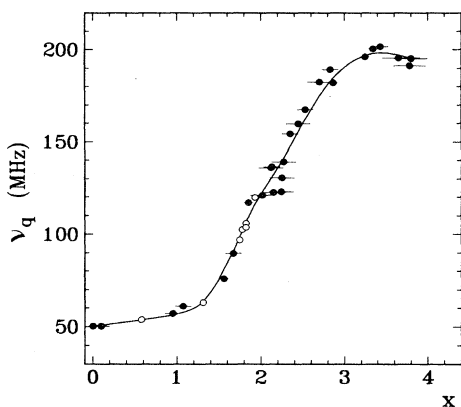
only the data of the fast-fluctuation regime can be used for the determination of the activation energy of the jump process. The slope of the high-temperature $(T > 270$ K) Arrhenius relation in Fig. 5 corresponds to an activation energy $E_a = 2180(120)$ K for HfV$_2$H$_{1.78}$.

The main results of this investigation are summarized in Figs. 6–9. For several concentrations, only the room-temperature frequency v_q(290 K) has been determined. The concentration dependence of v_q(290 K) is given in Fig. 6. The results for the asymmetry parameter η of the dominant fraction for the different hydrogen concentrations and temperatures are collected in Fig. 7, the corresponding values of the quadrupole frequency v_q are shown in Fig. 8. As the frequencies of the two fractions in the low-temperature spectra usually differ by less than 10%, only their mean value is displayed. The activation energies E_a for hydrogen jumps in HfV$_2$H$_x$, determined from the Arrhenius relation $\ln\lambda$ vs $1/T$ in the fast-fluctuation regime, are plotted in Fig. 9 as a function of the hydrogen concentration x.

VI. DISCUSSION

A. The quadrupole interactions in HfV$_2$ between 290 and 1760 K

A discussion of the unusual temperature dependence of the quadrupole frequency of ^{111}Cd in unloaded HfV$_2$ (see Fig. 3) has to address the question of the site occupied by the probe nucleus as an impurity in the C15 Laves phase. Although direct evidence for the occupied site is not available, the measured QI parameters strongly suggest that ^{111}Cd resides on a substitutional V site. From the fact that a single, well-defined QI rather than a distribution is observed we may conclude that the probe nuclei are on regular sites of the host lattice. Among the substitutional sites of the C15 structure, only the V site has the noncubic, axial point symmetry necessary to explain the observed axially symmetric QI. The substitutional Hf site can be excluded because its point symmetry is cubic
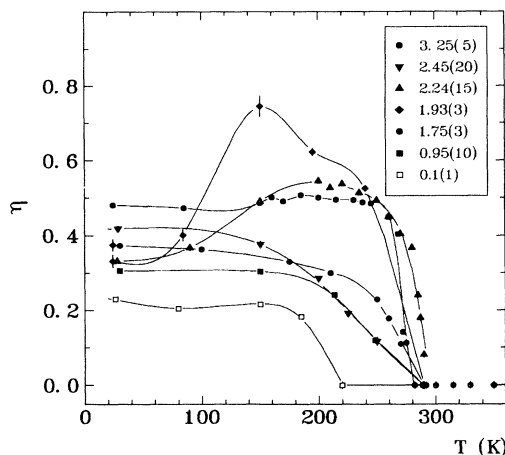

FIG. 6. The dependence of the room-temperature quadrupole frequency v_q(290 K) of ^{111}Cd:HfV$_2$H$_x$ on the hydrogen concentration x. The full points refer to samples annealed in a high vacuum system, the open points to samples annealed in ultrahigh vacuum.

FIG. 7. The temperature dependence of the asymmetry parameter η of the quadrupole interaction of ^{111}Cd:HfV$_2$H$_x$ at different hydrogen concentrations x.
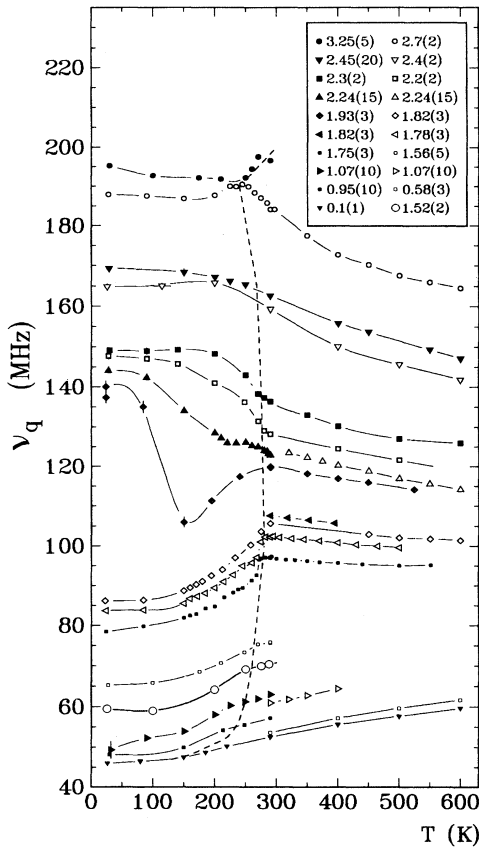
FIG. 8. The quadrupole frequency ν_q of ^{111}Cd:HfV$_2$H$_x$ as a function of temperature and hydrogen concentration x. The dotted line connects the $T_{\eta=0}$ points at the different concentrations. On the right of this line the EFG has axial asymmetry ($\eta=0$), on the left side the EFG is axially asymmetric ($\eta\neq0$).
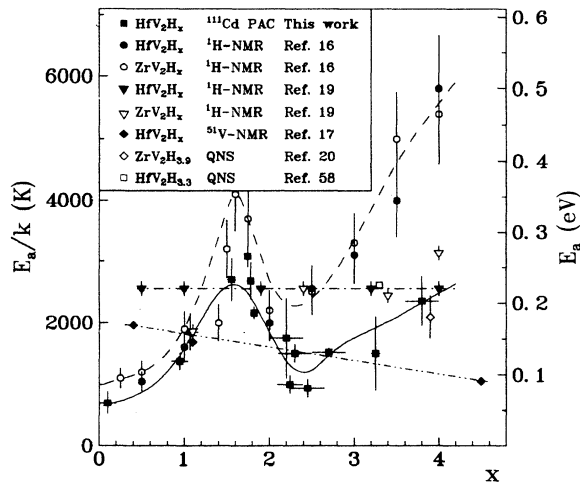
FIG. 9. The activation energy of the hydrogen diffusion in HfV$_2$H$_x$ and ZrV$_2$H$_x$ as a function of the hydrogen concentration x determined by PAC (this work), NMR (Refs. 16, 17, and 19) and QNS (Refs. 20 and 58). The different lines are drawn to guide the eye.

and the EFG therefore vanishes. This has been confirmed by PAC studies of HfV$_2$ with the probe ^{181}Ta which being populated in the decay of ^{181}Hf occupies the Hf site.[25,26] Among the interstitial sites, only the e-site symmetry (3V/1Hf) is compatible with an axially symmetric QI. In addition to the size aspect, an argument favoring the substitutional V site rather than the interstitial e site as the impurity location comes from the observation that the ratio of the EFG's V_{zz} (^{111}Cd)/V_{zz}(^{51}V)$=3.8(1.0)$ experienced by ^{51}V (Refs. 14, 17, and 24) and ^{111}Cd (Ref. 27) in HfV$_2$ is within the errors identical to the ratio of the Sternheimer corrections[46] of the two probes: $(1-\gamma_\infty)_{Cd}/(1-\gamma_\infty)_V=3.6$. This implies that the lattice contribution to the EFG is very similar in both cases which makes it quite likely that both probes have the same atomic environment and reside on the same site.

Apart from establishing the continuous increase of the QI up to the melting point of HfV$_2$ (Fig. 2), the measurements described in Sec. V A suggest the existence of a high-temperature modification of HfV$_2$. The temperature dependence of the relative amplitudes $f_i(i=1,2,3)$ of three sites detected in the PAC spectra by their different QI parameters (Fig. 3) clearly indicate that a transformation sets in at about 1200 K: above this temperature two new fraction f_2,f_3 appear in the spectra at the expense of the site with fraction f_1 which, dominating at low temperatures, can be associated with the MgCu$_2$-type structure of HfV$_2$. The samples can be heated up to $T=1650$ K without irreversible changes of the room-temperature spectra, as shown by the open squares in Fig. 3 which represent the room-temperature fraction $f_1(290$ K) observed after the respective high-temperature measurement. Only after heating to temperatures $T>1650$ K, the room-temperature fraction $f_1(290$ K) starts to decrease irreversibly, possibly due to the diffusion of the PAC probes towards grain boundaries. The changes observed in the PAC spectra between 1200 and 1650 K therefore quite probably reflect a transformation of the host lattice itself and are not related to the impurity nature of the probe ^{111}Cd. High-temperature PAC measurements with ^{181}Ta would be useful for a confirmation of this conclusion.

The rate of the transformation $f_1\rightarrow f_2,f_3$ can be roughly estimated from the decrease Δf_1 between two consecutive measurements. With $\Delta f_1\sim0.05-0.10$ for 1200 K $\leq T\leq1500$ K (see Fig. 3) and typical data collection times of 10 h for each temperature, one obtains a rate of the order of $5-10\times10^{-3}$ h^{-1}. So, thermal equilibrium is reached only very slowly which explains the large difference in the value of f_1 at $T=1450$ K measured after slow and fast heating, respectively, (full point and square, respectively, in Fig. 3).

The structure of the two sites appearing at high temperatures cannot be identified from their QI parameters alone. The broad frequency distribution of f_2 (see Sec. V A) suggests a considerable degree of disorder after the transformation in parts of the sample and the very weak interaction of f_3 may be an indication of a cubic environment. For a definite answer as to whether HfV$_2$ is po-

lymorphic, as suggested by Guzej et al.,[36] further studies using x ray diffraction, thermal analysis, and metallography appear necessary.

B. The concentration dependence of v_q(290 K) in HfV$_2$H$_x$

Hydrogenation of HfV$_2$ leads to an increase of the room-temperature quadrupole frequency v_q(290 K) of [111]Cd (Fig. 6). It should be recalled that at room temperature we are already in the region of fast fluctuations (see Figs. 4 and 5) and therefore the frequency derived from the oscillations of the PAC pattern corresponds to the time average of the QI. The most interesting aspect of Fig. 6 is the drastic change of the slope $\delta \ln v_q / \delta x$ at the hydrogen concentration $x \sim 1.5$. Below $x \sim 1.5$ v_q(290 K) increases only slightly with increasing x [$(\delta \ln v_q / \delta x)_{x=0} \approx 0.2$], above $x \sim 1.5$ one finds a strong, practically linear increase with slope $(\delta \ln v_q / \delta x)_{x=1.5} \approx 1.1$ which extends up to $x \sim 3.3$. At still higher concentrations v_q(290 K) remains almost constant, but at these concentrations HfV$_2$H$_x$ is no longer in the α phase. The discussion shall therefore be restricted to concentrations $x \leq 3.3$.

Qualitatively, the same trend of v_q(290 K) vs x has been observed in all investigations of the ^{51}V QI in HfV$_2$H$_x$ and ZrV$_2$H$_x$ reported up to now: According to Däumer, Khan, and Lüders[17] the ^{51}V QI in HfV$_2$H$_2$H$_x$ is constant up to $x \sim 1$ and increases strongly at higher concentrations with slope $(\delta \ln v_q / \delta x)_{x=1} \sim 0.5$. In the same compound Ding et al.[22] find a linear increase of v_q(290 K) with slope $(\delta \ln v_q / \delta x)_{x=1} \sim 0.8$ for $1 \leq x \leq 3$. Concentrations $0 < x < 1$ have not been studied by these authors. In ZrV$_2$H$_x$ (Ref. 21) the slope of the concentration dependence also changes at $x \sim 1$ from $(\delta \ln v_q / \delta x)_{x=0} \lesssim 1$ to $(\delta \ln v_q / \delta x)_{x=1.5} \sim 2.5$. In a NRM study of the ^{51}V QI in TaV$_2$H$_x$ ($0 \leq x \leq 1.54$) Skripov, Belyaev, and Stepanov[47] have observed a pronounced minimum of the QI at $x \approx 0.7$ with v_q coming close to zero. Since NMR (as standard PAC) is not sensitive to the sign of the QI, the authors propose that the minimum results from a change of sign of the EFG at $x \approx 0.7$. In this case the absolute value $|v_q|$ would be an almost linear function of the hydrogen concentration. Skripov, Belyaev, and Stepanov[47] then suggest that a change of sign might also occur at small hydrogen concentrations in HfV$_2$H$_x$ and ZrV$_2$H$_x$. Judging from the smooth increase of our $|v_q|$ data in the range $0 \leq x \leq 1.3$, a change of sign of the EFG in HfV$_2$H$_x$, although not impossible, appears very unlikely. Whatever arbitrary assumption on the sign of v_q is made, there is no way to produce a linear v_q vs T relation with the same slope as at high concentrations. One has to conclude that at low hydrogen concentrations the relative change of v_q is much smaller than at concentrations $x > 1.5$.

Based on the naive picture of a metal as a lattice of positively charged ions immersed into a sea of conduction electrons, the electric-field gradient (EFG) at nuclear sites in noncubic metals is frequently written as the sum of a lattice contribution V_{zz}^{lat}, enhanced by the Sternheimer effect, and a valence and conduction-electron contribu-

tion V_{zz}^{el}:

$$V_{zz} = (1 - \gamma_\infty) V_{zz}^{lat} + V_{zz}^{el} . \tag{6}$$

There is ample evidence from systematic experimental studies that the major contribution to the EFG in noncubic metals comes from the valence and conduction electrons.[30] In those cases where the sign of the EFG could be determined the electronic part V_{zz}^{el} was frequently found to be a factor of 2–3 larger than the enhanced lattice contribution calculated by a lattice sum and to have the opposite sign.[48] A lattice sum calculation for Cd on V sites of unloaded HfV$_2$ (see below) yields $(1 - \gamma_\infty) V_{zz}^{lat} = 1.7 \times 10^{17}$ V/cm^2. The comparison with the experimental EFG $V_{zz} = 2.5 \times 10^{17}$ V/cm^2 (calculated from v_q(290 K) = 51 MHz) shows that in case of opposite signs V_{zz}^{el} exceeds the lattice part here too by more than a factor of 2. Recently Blaha, Schwarz, and Dederichs[49] have carried out first-principles band-structure calculations of the EFG in hcp metals which agree well with the experimental data. These calculations also show that the EFG is mainly determined by the valence electron distribution, in particular the p-electron density, close to the probe nucleus.

Partitioning the EFG as in Eq. (6) is helpful for a qualitative discussion of the observed changes of the QI upon hydrogenation. Both contributions may be affected. If we assume, as suggested by the concentration dependence of the DOS at the Fermi energy,[7,17,18,32] that hydrogen in HfV$_2$H$_x$ is protonic, electrons transferred from the hydrogen to the valence and conduction-band influence the electronic part and the positive hydrogen ions generate an additional lattice contribution $V_{zz}^{lat}(H)$.

The concentration dependence of the time-averaged hydrogen sublattice contribution $V_{zz}^{lat}(H)$ can be estimated by a point-charge lattice sum calculation.[50] In spite of its limitations, the point-charge model is useful for a discussion of qualitative trends and may help to decide on the relative importance of the two terms in Eq. (6) for the observed variation of $\delta \ln v_q / \delta x$. We have assumed that as in ZrV$_2$H$_x$ only the g (2V/2Zr) and the e sites (3V/Zr) are occupied at concentrations $x < 3.3$ (Ref. 20) and have carried out the summation for the g- and e-site hydrogen sublattices, occupied with charges Q_g and Q_e, respectively. The calculation for the $C15$ structure yields $V_{zz}^{lat}(g) = -43 Q_g/e$ and $V_{ee}^{lat}(e) = +15 Q_e/e$ in units of $V_{zz}^{lat}(m) = 5.5 \times 10^{15}$ V/cm^2 with $\eta_g = \eta_e = 0$. $V_{zz}^{lat}(m)$ is the EFG produced by the metal-ion lattice of unloaded HfV$_2$, calculated for the ion charges Hf^{4+}, V^{2+} and the lattice parameter $a = 7.395$ Å.

A rapidly diffusing hydrogen ion spends the same amount of time on all N_i equivalent sites of type S_i of the hydrogen lattice so that in the time average the same charge $Q_i = Z'ep_i$ resides on all sites S_i. $Z'e$ is the effective charge of the jumping hydrogen ion and p_i the occupation probability of sites S_i. For only one type of site p_i given by $p_i = x/N_i$ and the time averaged charge Q_i increases linearly with the hydrogen concentration x. For more than one type of site, one has $x = \sum_i N_i p_i$.

We assume that the concentration dependence of the occupation probabilities of the g and e sites in ZrV$_2$H$_x$,

known from the work of Hempelman *et al.*,[20] also holds for HfV$_2$H$_x$: For $0 \leq x \leq 1.5$ the hydrogen resides on g sites only so that $p_g \approx 1/12x$ and $p_e \approx 0$. The e-site occupation sets in at $x \sim 1.5$ and in the range $1.5 < x < 3.3$ the occupation probabilities can be approximated by the linear relations $p_g = 0.035 + 0.06x$ and $p_e = 0.07(x-1.5)$. With these relations for $p_{g,e}(x)$, $Q_i = Z'ep_i$ and the above results of the lattice sum calculation one obtains for the concentration dependence of the total lattice EFG

$$V_{zz}^{\text{lat}}(x) = V_{zz}^{\text{lat}}(m) + V_{zz}^{\text{lat}}(g) + V_{zz}^{\text{lat}}(e)$$

in the two concentrations ranges:

$$0 \leq 0x \leq 1.5: \quad V_{zz}^{\text{lat}}(x) \approx V_{zz}^{\text{lat}}(m)(1 - 3.6Z'x) \;,$$

$$1.5 < x < 3.3: \quad V_{zz}^{\text{lat}}(x) \approx V_{zz}^{\text{lat}}(m)[1 - 1.5Z'(x+2)] \;.$$

So, according to this lattice sum calculation, the EFG contribution produced by the positively charged metal ions and protonic hydrogen on g and e sites decreases with increasing hydrogen concentration with slopes $(\delta \ln V_{zz}^{\text{lat}}/\delta x)_{x \leq 1.5} = -3.6Z'$ and $(\delta \ln V_{zz}^{\text{lat}}/\delta x)_{x > 1.5} = -1.5Z'$, respectively. The smaller slope at the higher hydrogen concentrations is the result of the opposite sign of the g- and e-site contributions and the onset of the e-site population at $x \sim 1.5$.

The effective hydrogen charge Z' (in units of e) can be estimated from the dynamical quadrupole frequency v_q^f, because it is the motion of the hydrogen ion which causes the fluctuations of the QI and the resulting PAC relaxation [see Eq. (4)]. The fact that the dynamical quadrupole frequency and the maximum value λ_k^{max} of the relaxation parameter obtained with the approximation of a single relaxation constant are approximately related by $\lambda_k^{\text{max}} \approx 1/2v_q^f$ (Refs. 43 and 51) may be used to determine v_q^f without knowledge of the residence time $\tau_R = 1/Nw$.

The value of λ_k^{max} varies with the hydrogen concentration from $\lambda_k^{\text{max}} \approx 3$ MHz at $x = 0.1$ through a maximum of $\lambda_k^{\text{max}} = 8(2)$ MHz in the range $1 \leq x \leq 2$ to $\lambda_k^{\text{max}} = 3(1)$ MHz at $x = 3.8$, giving a maximum of $v_q^f = 16$ MHz. As the static frequencies v_q^s at intermediate concentrations are of the order $v_q^s \approx 100-120$ MHz (see Fig. 8), one has $v_q^f/v_q^s \leq 0.15$. λ_k^{max} or v_q^f are expected to pass through a maximum because the probability for hydrogen jumps in the nearest-neighbor (NN) shell of the probe atom, which produce the dominant contribution to the averaged dynamical frequency v_q^f, depends on both the number of hydrogen ions and the number of vacant NN sites. At small concentrations there are few hydrogen ions, at large concentrations few NN vacancies.

The quadrupole frequency produced by a charge Z' at a distance r from a nucleus with quadrupole moment Q is given by $v_q = 2Z'eQ(1-\gamma_\infty)r^{-3}h$. Inserting $Q = 0.83b$ for the quadrupole moment of the 5/2 state of ^{111}Cd,[52] $(1-\gamma_\infty) = 31$ for the Sternheimer correction of Cd^{2+} and $r = 1.8$ Å for the distance between the V site and the nearest hydrogen site one obtains $v_q \approx 300Z'$ (MHz). The comparison of this value with the experimental value $v_q^f \approx 16$ MHz leads to an effective charge of $Z' \approx 0.05$ which is very similar to the hydrogen charge in ScH$_2$ ($Z' = 0.06$) determined by Han *et al.*[53]

With $Z' = 0.05$ the decrease of the lattice contribution for concentrations $x > 1.5$ is given by $(\delta \ln V_{zz}^{\text{lat}} \delta x)_{x > 1.5} = -0.075$. So, even under the most favorable assumptions (opposite sign of V_{zz}^{lat} and V_{zz}^{el} and $|V_{zz}^{\text{el}}| > |V_{zz}^{\text{lat}}|$) the decrease of V_{zz}^{lat} with increasing x can at best account for about 10% of the experimentally observed increase of v_q(290 K) in the range $1.5 < x < 3.3$ ($\delta \ln v_q/\delta x = 1.1$). The estimated charge is of course subject to some uncertainty, but it would require an unrealistically large value of $Z' \sim 1$ to explain the experimental value of $\delta \ln v_q/\delta x$ with the variation of $V_{zz}^{\text{lat}}(x)$ alone. And even with $Z' \sim 1$, the calculation predicts—due to the e-site population—a decrease of $\delta \ln v_q/\delta x$ at higher concentrations which is in conflict with the experimental observation.

These considerations suggest that the observed concentration dependence of v_q(290 K) mainly reflects the variation of the electronic part V_{zz}^{el} of the EFG, caused by the filling of the valence and conduction bands with electrons provided by the hydrogen. Only a minor contribution comes from the time-averaged EFG produced by rapidly diffusing protonic hydrogen on g and e sites.

This conclusion then implies that the effect of the electron transfer on the EFG changes drastically with the position of the Fermi energy in the DOS curve. As pointed out above, $N(E_f)$ decreases steeply when the Fermi energy is shifted upwards by hydrogenation. For concentrations $0 < x < 1.5$, with E_f in the region of a large DOS, the addition of electrons leaves the EFG practically unchanged whereas for $x > 1.5$, with E_f in the DOS valley, the increase of the electron density produces a strong increase of the EFG. Now, the band-structure calculations[7,8] and the ^{51}V Knight-shift data for HfV$_2$H$_x$ (Ref. 17) show that the high DOS comes mainly from the V d orbitals so that at low concentrations $0 < x < 1.5$ the electrons introduced by hydrogenation predominantly occupy the V d states. The observation that although we increase the electron density in the V d subband the QI at the V site remains almost constant then leads to the conclusion that the EFG produced by the d-electron charge distribution must be small compared to the contributions of other subbands. This agrees with the first-principles calculation of the EFG in hcp metals by Blaha, Schwarz, and Dederichs[49] who show that the dominant EFG contribution comes from the p-valence electrons. According to these calculations the d-electron distribution plays a minor role, even for transition metals. The steep increase of the EFG for $x > 1.5$ can then be related to the decreasing partial DOS of the V d subband. When the V d states no longer dominate the DOS, the electron density in the V p band and thus the EFG at the V site may increase with the hydrogen contents. The band-structure calculations show that while in the region of the DOS peak, the density of V d states exceeds that of the p states by almost a factor of 10, both are of the same order of magnitude in the DOS valley.[7,8]

So, in our opinion the pronounced change in the relative concentration dependence of the QI at $x \approx 1.5$ is a consequence of the particular band structure of HfV$_2$ and strongly points to the p-valence electron distribution at

the V site as the dominant source of the EFG of ^{111}Cd in HfV$_2$H$_x$.

C. The temperature dependence of the quadrupole interaction in HfV$_2$H$_x$ at different hydrogen concentrations

The temperature dependence of the QI of ^{111}Cd in HfV$_2$H$_x$ is described in Figs. 7 and 8 by the asymmetry parameter $\eta(T;x)$ and the quadrupole frequency $\nu_q(T;x)$, respectively. In those cases where two sites were required for a description of the low-temperature spectra the average frequency and the asymmetry of the dominant site are shown.

At all hydrogen concentrations we find a finite asymmetry parameter at low temperatures which, however, shows no obvious systematic dependence on the hydrogen contents. Qualitatively, the finite asymmetry is compatible with the orthorhombic and tetragonal symmetry of the low-temperature phases and in part also related to the static, low-temperature QI distribution which results from the statistical distribution of the hydrogen on the available interstitial sites; the average asymmetry parameter of an EFG distribution is finite and increases with the distribution width, even if the symmetry of the perfect crystal corresponds to $\eta=0$.[54] A quantitative discussion of the temperature dependence of η at different concentrations, as carried out in Ref. 28 for the case of ^{111}CdHfV$_2$H$_4$, however, requires more details on the structure, the hydrogen sites, and the temperature variation of the lattice parameters of the low-temperature phases than presently available. The temperature $T_{\eta=0}$ at which η vanishes marks an upper limit of the transition temperature to the $C15$ structure (α phase) of HfV$_2$H$_x$. The transition may occur at temperatures $T<T_{\eta=0}$ because the hydrogen distribution produces some asymmetry even if the host has axial symmetry.[54] Therefore the slow variation of $T_{\eta=0}$ with the hydrogen concentration x, shown by the dotted line in the ν_q vs T plot of Fig. 8, is not in conflict with the pronounced concentration dependence of the α-phase boundary in the T-x phase diagram of ZrV$_2$H$_x$.[20]

A discussion of the quadrupole frequency ν_q and its variation at low temperatures, i.e., left of the $T_{\eta=0}$ line in Fig. 8, is difficult because of the limited knowledge on the structure of the low-temperature phases at different hydrogen concentrations. Qualitatively one notes a strong increase in ν_q(24 K) between $x=1.82$($\nu_q\approx97$ MHz) and $x=2.24$($\nu_q\approx145$ MHz) and a change in the temperature trend of ν_q in the same concentration range. For $x\leq1.83$ ν_q increases, for $x>1.90$ ν_q decreases with temperature towards the $T_{\eta=0}$ line. The large difference in the low-temperature frequencies suggests different structures and thus a phase boundary between $x=1.82$ and 2.24, in agreement with the ZrV$_2$H$_x$ T-x phase diagram[20] which places the lower limit of the homogeneity range of the fct β phase at $x\approx2$. At $x=1.93$ both phases contribute to the PAC spectrum (see Sec. V B). At 24 K the high-frequency component, which probably represents the β phase, dominates; with increasing temperature it decreases continuously, feeding the low-frequency frac-

tion which suggests a second-order phase transition and explains the minimum of the average frequency of HfV$_2$H$_{1.93}$ at $T\approx150$ K in Fig. 8.

The right side of the $T_{\eta=0}$ line in Fig. 8 is a single-phase field, showing the frequencies in the α phase of the HfV$_2$H$_x$ system as a function of temperature for different hydrogen concentrations. The remarkable aspect of these data is the observation that the sign of the temperature derivative $(\delta\ln\nu_q/\delta T)_{T>300\text{ K}}$ changes with the hydrogen concentration and that again the position of the Fermi energy on the DOS appears to be a decisive parameter in this context. At small hydrogen concentrations, with E_f in the peak region of the DOS, the quadrupole frequency increases with temperature. But as the concentration increases and E_f moves towards the DOS valley, the QI at first becomes almost temperature independent (see $x\approx1.75$) and finally decreases with temperature.

If we exclude the possibility of a fortuitous coincidence, this behavior suggests a strong influence of the Fermi-surface electrons on the temperature behavior of the EFG. Apparently, this contribution increases with temperature and where the density of Fermi surface electrons is high, it can overcome the usual effects of thermal expansion and lattice vibrations. Watson, Gossard, and Yafet[55] pointed out that Fermi-surface electrons may contribute to the temperature dependence of the EFG because, when temperature is raised, electrons can be excited to states of different orbital symmetry above the Fermi level. The effect of this thermally induced repopulation depends on the details of the band structure and is difficult to evaluate but the prediction that the EFG of the transition metals Hf, Ru, and Y should increase with temperature[56] shows that conditions may exist where the thermal repopulation overcomes the decrease caused by lattice expansion and thermal vibrations.

We have argued above that in the present case the V p electrons are the main source for the EFG at the V site and that the contribution of the V d electrons which dominate the DOS at small hydrogen concentrations is rather small. In this picture the EFG would increase with temperature if the repopulation of "ineffective" d electrons into p states produces an increase of the V p electron density.

The sign and magnitude of the changes in the p- and d-electron density at the V site by thermal excitation depends on the detail of the band structure. For a qualitative discussion, we have calculated the temperature derivative $\delta n_p/\delta T$ of the p-electron density at the Fermi energy for the simplifying case that the total DOS $N(E)$ consists of only two rigid subbands, p electrons with partial DOS $N_p(E)$ and density n_p and d electrons with partial DOS $N_d(E)$ and density n_d, respectively. With the condition that the total electron density $n=n_p+n_d$ is temperature independent, standard procedures[57] involving a Taylor expansion of N_p and N_d about the Fermi energy to the first term lead to the expression

$$\frac{dn_p}{dT}\bigg|_{E_F\gg kT}=\frac{\pi^2}{3}k^2T\frac{N_dN_p}{N}\left[\frac{\delta\ln N_p}{\delta E}-\frac{\delta\ln N_d}{\delta E}\right]\bigg|_{E=E_F}.$$

(7)

So, with E_f located in a region of negative energy derivatives of the DOS as in HfV_2, an increase of the p density by thermal repopulation requires that the p DOS decreases slower with energy than the d DOS which agrees with the expectation based on the principle of the minimum energy. At present, one has no experimental data to decide whether this condition is fulfilled for HfV_2. However, the above expression shows that thermal repopulation effects can be expected preferentially in regions of large, rapidly varying DOS. The observation that the range $0 \leq x \leq 1.5$ of the anomaly $\delta \ln v_q / dT > 0$ coincides with the region of strongly decreasing DOS (Refs. 17,18, and 32) therefore supports the interpretation that the positive sign of $\delta \ln v_q / dT$ results from a repopulation of Fermi-surface electrons. A confirmation of this picture by *ab initio* calculations of the EFG as a function of temperature would be of great interest.

D. The activation energy E_a of the hydrogen diffusion in HfV_2H_x

Figure 9 shows the activation energy E_a of the hydrogen diffusion in HfV_2H_x, determined from the $\ln \lambda$ vs $1/T$ plot in the fast-fluctuation region (see Sec. V B) as a function of the hydrogen concentration x. These PAC results are compared to the values obtained by NMR measurements of the spin relaxation of ^1H in HfV_2H_x and ZrV_2H_x (Refs. 16 and 19) and of ^{51}V in HfV_2H_x (Ref. 17) and by measurements of quasielastic neutron scattering (QNS) in $ZrV_2H_{3.9}$ (Ref. 20) and $HfV_2H_{3.3}$.[58]

Skripov et al.[19] have studied the hydrogen diffusion separately in the phases with an ordered (low temperature) and a disordered (high temperature) H sublattice, respectively, and could confirm the previous PAC observation[28] that hydrogen ordering results in an increase of the residence time between diffusion jumps. For the disordered α phase of HfV_2H_x, Skripov et al.[19] obtained the same activation energy $E_a = 0.22(1)$ eV at all concentrations and for α-ZrV_2H_x these authors found a slight increase of $E_a(x)$ from $E_a(1.1) = 0.16$ eV to $E_a(4.0) = 0.27$ eV, followed by a sharp decrease to $E_a(5.0) = 0.17$ eV. In contrast to the results of Skripov et al.,[19] Shinar, Davidov, and Shaltiel[16] report for ZrV_2H_x the existence of a peak in E_a at about $x = 1.6$ and for both ZrV_2H_x and HfV_2H_x a strong increase of E_a at $x > 2$ (see broken line in Fig. 9). According to Skripov et al.,[19] the discrepancy between these ^1H NMR experiments results from an inadequate data analysis by Shinar, Davidov, and Shaltiel[16] who have neglected the effect of the order-disorder transition on the diffusion parameters. The ^{51}V measurements for HfV_2H_x give still another $E_a(x)$ dependence; Däumer, Khan, and Lüders[17] find a decrease of E_a from $E_a(0.4) = 0.169$ eV to $E_a(4.5) = 0.091$ eV.

Our ^{111}Cd PAC results (full squares, connected by the full line in Fig. 9) show a pronounced concentration dependence of the activation energy which resembles the trend reported by Shinar, Davidov, and Shaltiel,[16] although the absolute values at high concentrations differ considerably. Starting at low concentrations, we first find an increase of E_a towards a peak at $x \approx 1.5$, which is fol-

lowed by a decrease towards a minimum at $x \approx 2.4$ and another increase to higher concentrations. The PAC result for $x = 1$ agrees well with the ^1H NMR value of Shinar, Davidov, and Shaltiel[16] and the ^{51}V NMR value[17] which are all considerably smaller than the ^1H NMR value of Skripov et al.[19] At $x = 3.8$ the PAC value agrees with the ^1H NMR value of Skripov et al.[19] and the QNS value for $ZrV_2H_{3.9}$,[20] whereas the ^1H NMR value of Shinar, Davidov, and Shaltiel[16] in this concentration range is much larger and the ^{51}V value[17] much smaller.

In view of the pronounced difference between the ^1H NMR result of Skripov et al.[19] and our PAC result for the $E_a(x)$ dependence, the question of possible systematic uncertainties of the analysis must be discussed. Only PAC measurements in the disordered α phase and the fast-fluctuation region have been used for the determination of E_a. Therefore an influence of order-disorder transitions on the PAC result can be excluded. The measurements have been analyzed with an approximation of the Blume theory [Eq. (3)], the validity range of which has been carefully investigated[43] and it has been established beyond doubt that in the fast fluctuation region the approximation maintains the relation $\lambda_k \propto (v_q^f)^2 / w$ between the relaxation parameter and the jump rate w, even for weak fluctuating interactions v_q^f as in the case of low concentrations [see Eq. (4)]. For Arrhenius processes one then has $\delta \ln \lambda_k / \delta(1/T) \propto E_a / k + 2\delta \ln v_q^f / \delta(1/T)$. Therefore, in principle, a temperature dependence of the fluctuating QI influences the value of E_a derived from the temperature dependence of the relaxation parameter, but the effect is small: A decrease of v_q^f by 10% between 250 and 500 K corresponds to $2\delta \ln v_q^f / \delta(1/T) = -100$ K, which is to be compared to activation energies of $E_a \approx 1$–3×10^3 K. Therefore the analysis of the PAC measurements can be considered free of systematic uncertainties. There is, however, one important difference between ^1H NMR and the PAC technique: While ^1H NMR measures the hyperfine interaction seen by the jumping proton itself, PAC involves a fixed probe nucleus which—as in the present case—is frequently an impurity in the investigated system. Because of the r^{-3} dependence of the QI, a fixed probe detects only charges jumping in its neighborhood and as the potential in the vicinity of an impurity site may differ from that of the regular lattice sites, it can *a priori* not be excluded that in the case of impurity probes the barrier height measured by the PAC technique is affected by the impurity itself. This effect may possibly lead to a difference in the absolute value of the activation energy determined by PAC and ^1H NMR, but as the PAC impurities in the present experiment are highly dilute (≤ 1 ppm) we would not expect that the concentration dependence of the activation energy is affected. For more information on this question, we are presently carrying out PAC experiments with different impurity probes in the same metal hydride.

VII. SUMMARY

In this paper we have presented a perturbed-angular-correlation study of the static and dynamic electric quad-

rupole interaction of the nuclear probe ^{111}Cd on V sites of the $C15$ Laves-phase hydrides HfV$_2$H$_x$ as a function of temperature and hydrogen concentration x. The main results and conclusions of this investigation are the following.

(i) It has been established that the anomalous increase of the ^{111}Cd quadrupole frequency v_q in unloaded α-HfV$_2$ with temperature, previously observed for $T \leq 900$ K,[27] continues up to the melting point of the compound.

(ii) The PAC spectra reflect a reversible structure transformation in the temperature range 1200–1500 K which suggests that HfV$_2$ is possibly polymorphic.

(iii) The room-temperature quadrupole frequency in α-HfV$_2$H$_x$ increases with the hydrogen concentration x. The increase can be approximated by two linear functions with a drastic change of slope at $x \approx 1.5$: $(\delta \ln v_q / \delta x)_{x=0} \approx 0.2$ and $(\delta \ln v_q / \delta x)_{x=1.5} \approx 1.1$. This observation can be related to the high density of V d states at the Fermi energy of HfV$_2$H$_x$ in the concentration range $0 \leq x \leq 1.5$ and points to the p-valence elec-

trons as the dominant source of the electric-field gradient at the V site of HfV$_2$H$_x$.

(iv) The variation of the quadrupole frequency in α-HfV$_2$H$_x$ with temperature depends sensitively on the hydrogen concentration x. For $x \leq 1.5$ one finds the same anomalous increase with temperature $\delta \ln v_q / \delta T > 0$ as in unloaded α-HfV$_2$, whereas at higher concentrations v_q shows the usual decrease $\delta \ln v_q / \delta T < 0$. The range of the anomaly $\delta \ln v_q / \delta T > 0$ coincides with a region of large, rapidly decreasing density of states in the band structure of HfV$_2$H$_x$ which supports the idea that the anomaly results from a thermal repopulation of Fermi-surface electrons.

(v) The activation energy E_a for hydrogen jumps in HfV$_2$H$_x$, derived from the dynamical damping of the PAC spectra in the fast-fluctuation regime, shows a maximum at intermediate concentrations $x \approx 1.5$ which is partially in conflict with the results of NMR measurements.

---

*On leave of absence from Department of Physics, Panjab University, Chandigarh, India.

[1] A. C. Lawson, Phys. Lett. 36A, 8 (1971).

[2] H. Zachariasen, Phys. Lett. 38A, 1 (1972).

[3] J. W. Hafström, G. S. Knapp, and A. T. Aldred, Phys. Rev. B 17, 2892 (1978).

[4] H. Takei, M. Yamawaki, A. Oota, and S. Noguchi, J. Phys. F 15, 2333 (1985).

[5] H. Keiber, C. Geibel, B. Renker, H. Rietschel, H. Schmidt, H. Wühl, and G. R. Stewart, Phys. Rev. B 30, 2542 (1984).

[6] B. Lüthi, M. Hermann, W. Assmus, H. Schmidt, H. Rietschel, W. Wühl, U. Gottwick, G. Sparn, and F. Steglich, Z. Phys. B 60, 387 (1985).

[7] B. M. Klein, W. E. Pickett, D. A. Papaconstantopoulos, and L. L. Boyer, Phys. Rev. B 27, 6721 (1983).

[8] M-C. Huang, H. J. F. Jansen, and A. J. Freeman, Phys. Rev. B 37, 3489 (1988).

[9] M. Gupta and L. Schapbach, in Topics of Applied Physics: Hydrogen in Intermetallic Compounds I, edited by L. Schlapbach (Springer, Berlin, 1988), Vol. 63, p. 139.

[10] A. Pebler and E. A. Gulbranson, Trans. Metall. Soc. AIME 239, 1593 (1967).

[11] P. Duffer, D. M. Dualtieri, and V. U. S. Rao, Phys. Rev. Lett. 37, 1410 (1976).

[12] J. J. Didisheim, K. Yvon, P. Fischer, and D. Shaltiel, J. Less-Common Met. 73, 335 (1980).

[13] A. V. Irodova, A. P. Glazkov, A. Somenkov, and S. Sh. Shilstein, J. Less-Common Met. 77, 89 (1981).

[14] H. Saji and T. Yamadaya, Phys. Lett. 39A, 359 (1972).

[15] J. Shinar, J. Less-Common Met. 104, 125 (1984).

[16] J. Shinar, D. Davidov, and D. Shaltiel, Phys. Rev. B 30, 6331 (1984).

[17] W. Däumer, H. R. Khan, and K. Lüders, Phys. Rev. B 38, 4427 (1988).

[18] A. P. Stepanov, A. V. Skripov, and M. Yu. Belyaev, Z. Phys. Chem. Neue Folge 163, 603 (1989).

[19] A. V. Skripov, M. Vu. Belyaev, S. V. Rychkova, and A. P. Stepanov, J. Phys. Condens. Matter 3, 6277 (1991).

[20] R. Hempelmann, D. Richter, O. Hartmann, E. Karlsson, and R. Wäppling, J. Chem. Phys. 90, 1935 (1989).

[21] M. Peretz, J. Barak, D. Zamir, and J. Shinar, Phys. Rev. B 23, 1031 (1981).

[22] D. T. Ding, J. I. de Lange, T. O. Klassen, N. J. Poulis, D. Davidov, and J. Shinar, Solid State Commun. 42, 137 (1982).

[23] M. Yu. Belyaev, A. V. Skripov, V. N. Kozhanov, and A. P. Stepanov, Sov. Phys. Solid State 26, 1285 (1984).

[24] M. Yu. Belyaev, A. V. Skripov, A. P. Stepanpv, M. E. Kost, and L. N. Paduretz, Sov. Phys. Solid State 28, 1538 (1986).

[25] H. C. Jain and M. A. A. Saad, Phys. Lett. 96A, 419 (1983).

[26] R. Heidinger, P. Perotto, and S. Choulet, Solid State Commun. 47, 283 (1983).

[27] H. C. Jain, L. Freise, and M. Forker, J. Phys. Condens. Matter 1, 2137 (1989).

[28] M. Forker, W. Herz, and D. Simon, Z. Phys. Chem. Neue Folge 163, 91 (1989).

[29] M. Forker, W. Herz, and D. Simon, J. Phys. Condens. Matter. 4, 213 (1992).

[30] R. Vianden, Hyperfine Interact. 35, 1079 (1987).

[31] K. Nishiyama, F. Dimmling, Th. Kornrumpf, and D. Riegel, Phys. Rev. Lett. 37, 357 (1976).

[32] C. Geibel, W. Goldacker, H. Keiber, V. Oestreich, H.Rietschel, and H. Wühl, Phys. Rev. B 30, 6363 (1984).

[33] O. Kubacheswski-von Goldbeck, At. Energy Rev. 8, 57 (1981).

[34] R. Rudy and S. Windisch, J. Less-Common Met. 59, 13 (1968).

[35] Yu. A. Kocherzhinskij, V. Ya. Markiv, and V. V. Pet'kov, Russ. Metall. 134, (1973).

[36] L. S. Guzej, E. M. Sokolovskaja, I. G. Sokolova, I. E. Belyaeva, G. N. Ronani, and S. M. Kuznetsova, Vestn. Mosk Univ. Khim. 23, 52 (1968); Chem. Abstr. 69, 100 177 (1968).

[37] R. Ferro and R. Marazza, At. Energy Rev. 8, 121 (1981).

[38] A. C. Lawson and W. H. Zachariasen, Phys. Lett. 38A, 1 (1972).

[39] V. N. Kozhanov, Y. P. Romanov, S. V. Verkhovskij, and A. P. Sterpanov, Phys. Met. Metall. 48, 108 (1981).

[40] H. Frauenfelder and R. M. Steffen, in Perturbed Angular Correlations, edited by E. Karlsson, E. Matthias, and K. Siegbahn (North-Holland, Amsterdam, 1963).

[41] M. Blume, Phys. Rev. 174, 351 (1968).

[42]H. Winkler and E. Gerdau, Z. Phys. **262**, 363 (1973).

[43]M. Forker, W. Herz, and D. Simon, Nucl. Instrum. Methods Phys. Res. Sect. A **337**, 534 (1994).

[44]A. Abragam and R. V. Pound, Phys. Rev. **92**, 943 (1953).

[45]M. Forker, W. Herz, U. Hütten, M. Müller, R. Müßeler, J. Schmidberger, D. Simon, A. Weingarten, and S. C. Bedi, Nucl. Instrum. Methods Phys. Res. Sect. A **327**, 456 (1993).

[46]F. D. Feiock and W. R. Johnson, Phys. Rev. **187**, 39 (1969).

[47]A. V. Skripov, M. Yu. Belyaev, and A. P. Stepanov, Solid State Commun. **71**, 321 (1989).

[48]R. S. Raghavan, E. N. Kaufmann, and P. Raghavan, Phys. Rev. Lett. **34**, 1280 (1975).

[49]P. Blaha, K. Schwarz, and P. H. Dederichs, Phys. Rev. B **37**, 2792 (1988).

[50]F. W. de Wette, Phys. Rev. **123**, 103 (1961).

[51]A. Baudry and P. Boyer, Hyperfine Interact. **25**, 803 (1987).

[52]P. Herzog, K. Freitag, M. Reuschenbach, and H. Walitzki, Z. Phys. A **294**, 13 (1980).

[53]J. W. Han, C. T. Chang, D. R. Torgeson, E. F. W. Seymour, and R. G. Barnes, Phys. Rev. B **36**, 615 (1987).

[54]M. Forker, Nucl. Instrum. Methods **106**, 121 (1973).

[55]R. E. Watson, A. C. Gossard, and Y. Yafet, Phys. Rev. **140**, A375 (1965).

[56]M. Piecuch and Ch. Janot, Hyperfine Interact. **5**, 69 (1977).

[57]N. W. Ashcroft and N. D. Mermin, *Solid State Physics* (Holt, Rhinehart and Winston, New York, 1976).

[58]R. L. Havill, J. M. Titmann, M. S. Wright, and M. A. Crouch, Z. Phys. Chem. Neue Folge **164**, 1083 (1989).